F2006V124

RIDE SIMULATIONS OF A HALF-CAR WITH A HYDRAULICALLY INTERCONNECTED PASSIVE SUSPENSION

Smith, Wade*, Zhang, Nong, Jeyakumaran, Jeku
Mechatronics and Intelligent Systems, Faculty of Engineering, University of Technology, Sydney, Australia

KEYWORDS - Vehicle dynamics, ride comfort, suspension modelling, interconnected suspension, simulation

ABSTRACT - In this paper, the development of a hydraulically interconnected suspension (HIS) system model and the integration of this model into a four degree-of-freedom half-car system is briefly introduced. The appropriate frequency response functions are derived in order to simulate the system response to a stochastic road profile. The sprung mass vertical and roll accelerations, the dynamic normal tyre force, and the suspension deflection are considered in the frequency domain up to 20 Hz. The simulated responses of two equivalent half-car models with conventional independent suspensions are also provided for comparison. The results indicate that HIS systems provide a potentially viable method by which to partially overcome the ride/handling compromise.

INTRODUCTION

Suspension systems can play a key role in enhancing vehicle safety. For example, well designed suspensions can greatly reduce vehicular rollover propensity by minimising vehicle roll rates during extreme manoeuvres. However, these improvements usually come at a cost. A vehicle with a relatively stiff suspension is likely to possess good handling stability but poor ride comfort, and vice versa. This ride/handling compromise has been addressed in a variety of ways. One such approach is through the use of hydraulic or mechanical interconnections between the individual wheel stations (spring-damper elements). An *interconnected suspension* system is one in which a displacement at one wheel station can produce forces at other wheel stations [1].

The main advantage of interconnecting wheel stations is that the suspension designer can achieve more control over the stiffness and damping of each suspension mode, instead of being entirely reliant upon single-wheel stiffness and damping to implicitly define modal characteristics. The exact arrangement and method of interconnection determines the degree to which individual modes can be controlled. In recent experimental studies, vehicles with hydraulically interconnected suspension (HIS) systems have displayed significantly improved handling capability in comparison to their non-interconnected 'equivalents' [2, 3]. However, the ride comfort performance of these HIS systems is a topic which, to the authors' knowledge, has not yet been investigated in the public domain.

In this paper, such an investigation of a 'typical' HIS vehicle's ride performance is conducted. The study focuses on the sprung mass response to road roughness in the important frequency range from 0 to 20 Hz, and comparison is made between the HIS vehicle and two 'equivalent' vehicles with conventional independent suspensions. The dynamic normal tyre force and suspension strut deflection are also considered to illustrate the broader effects of road roughness on each system's response.

SYSTEM DESCRIPTION

Vehicle ride performance is often investigated theoretically using a quarter-car model, but this would obviously be too simple to illustrate interconnected suspension principles, where multiple wheel stations are inherently required. In an effort to retain simplicity, whilst still accounting for fluid interconnections between wheel stations, a lumped-mass four-degree-of-freedom half-car model is used in this investigation. Numerical simulations of a similar full-car model show that the half-car simplification is capable of capturing the essential dynamics of the system [4]. The half-car, shown in Figure 1, is described by typical passenger vehicle parameters and consists of linear tyre damping and springing, linear conventional suspension springing, and a typical roll-plane HIS system, similar in arrangement to that studied by Liu [5]. The system inputs are the road displacements at both tyre contact 'points' and the system outputs are the vertical displacements of the unsprung masses and the vertical and roll displacements of the sprung mass.

The hydraulic system consists of: a double-acting cylinder at each wheel-station; hydraulic interconnection between the cylinders; and gas-filled accumulators and dampers, which provide the desired levels of springing and damping. The hydraulic circuits are arranged such that motion in a certain vehicle mode produces a nominal flow distribution which operates particular accumulators and dampers. The arrangement considered here may be described as *anti-oppositional* [6], meaning that stiffness is added to the vehicle roll mode without significantly affecting the bounce mode.

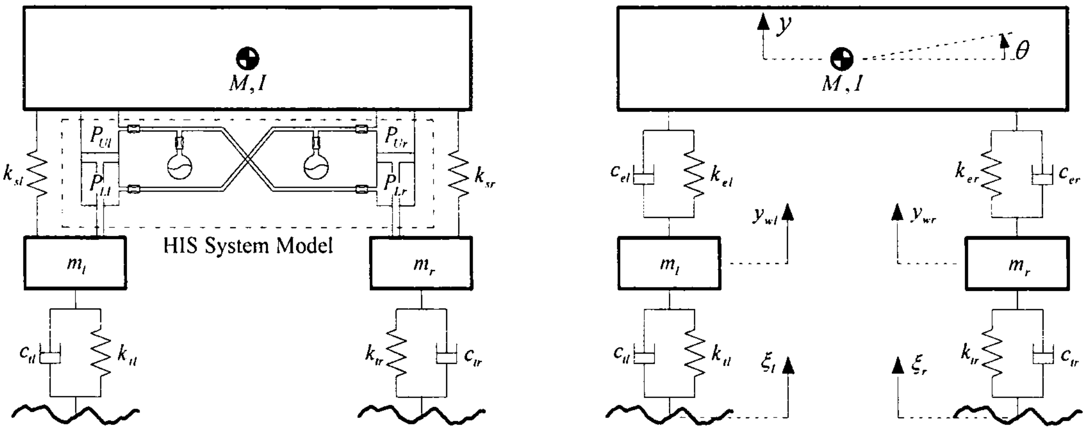

Figure 1: Layout of half-car with: an HIS (left); a conventional independent suspension (right)

HIS systems might appear prima facie to have similar characteristics to anti-roll bars, yet there are a number of noteworthy conceptual differences between the two. First, HIS systems (depending on the specific arrangement) have the capability not only to add roll *stiffness*, but also to add roll *damping*. Thus the roll damping ratio may be held constant with the addition of roll stiffness, a feature of which conventional anti-roll bars are not readily capable. Second, HIS systems can add roll stiffness without significantly affecting the roll moment distribution, which is crucial for directional response and handling performance. Third, HIS systems have the broader capability, at least ideally, to independently control four-wheel vehicle modes [1]. For example, increased roll stiffness and decreased articulation stiffness may be achieved simultaneously, which is unachievable with an anti-roll bar.

In addition to the HIS vehicle, Figure 1 also contains an 'equivalent' conventional independent suspension vehicle. The model is identical to that of the HIS vehicle, except that the suspension springs and double-acting cylinders are replaced with 'equivalent' linear springs and dampers. Both vehicles shown in the figure possess right-left symmetry, although this is not a requirement of the techniques henceforth employed. The equivalent stiffness and damping coefficients are determined as follows:

1. Free vibration analysis of the HIS vehicle is conducted [7].
2. The natural frequencies and damping for the bounce and roll modes are determined – the roll frequency is significantly higher than the bounce frequency due to the HIS system's added roll stiffness.
3. The stiffness and damping coefficients of the conventional suspension model are adjusted via a free vibration iterative process until the bounce and roll mode complex frequencies are 'matched' to those of the HIS vehicle.
4. Two sets of suspension stiffness and damping pairs (k_e, c_e) are thus obtained, which give equivalent modal properties to that of the HIS system – the parameters for the bounce mode vehicle are much lower (softer), than those for the roll mode vehicle.

The aim of this study is to compare the dynamic performance – particularly ride comfort – of these three vehicles, hereafter termed 'HIS', 'equivalent bounce', and 'equivalent roll'. We shall note briefly that the term *equivalent* is applied loosely and is not intended to imply literal equivalence. Indeed, as we shall see in the system equations introduced in a later section, the HIS vehicle possesses frequency-dependent stiffness and damping, which renders its exact modal duplication unattainable with the conventional suspension.

PERFORMANCE INDICES AND METHODS OF EVALUATION

Dynamic performance indices are a common tool employed to evaluate and/or optimise suspension system performance. The indices are usually set in the context of simplified quarter-car models and are based on mean square or root mean square (RMS) vehicle response to specified inputs. The most widespread of the considered response variables are the sprung mass vertical acceleration, the dynamic normal tyre force, and the relative displacement in the suspension strut [8], all of which are desirable to minimise. These responses are used to gauge, respectively, vehicle ride comfort, road holding, and suspension working space.

Here, since a half-car model is studied, vehicle ride comfort is assessed not only by sprung mass vertical acceleration, but also by sprung mass roll acceleration. Both acceleration responses are considered in terms of their Power Spectral Densities (PSDs) and are weighted according to human sensitivity, as described by ISO 2631-1 [9]. The aforementioned road holding and working space indicators are also assessed in their PSD forms.

Based on vehicle response to a specified road disturbance, the four performance indices for the three vehicles are compared qualitatively via response plots, rather than quantitatively via mean square or RMS values, although quantitative RMS-based performance evaluation would be a straightforward task.

The HIS vehicle is modelled by linearisation about the mean operating conditions, and advantage is taken of the three vehicles' linearity by considering system performance in the frequency domain, which is a convenient but non-essential approach.

No attempt is made here to investigate the handling performance of each vehicle. Some experimental studies have previously been conducted in that regard [2, 3], so this paper begins with the presupposition that interconnected schemes have the capability to deliver handling improvements. A theoretical examination of this hypothesis would require a more detailed vehicle model with the inclusion of parameters relevant to the vehicle's *lateral* dynamics. The road holding indicator employed herein must therefore be interpreted with caution since it is based on the tyre force due only to *vertical* dynamics, and consequently excludes important low frequency handling phenomena, such as the lateral load transfer resulting from vehicle roll. However, higher frequency, purely vertical dynamic tyre force fluctuation has been found to have an adverse effect on vehicle handling potential [10], so its application here is not without purpose.

ROAD SURFACE DESCRIPTION AND VEHICLE RESPONSE

Road profiles in vehicle dynamics modelling are generally treated as either deterministic (bumps, potholes etc.) or stochastic (random road roughness) processes [11]. Here, the latter approach is adopted. A completely random road profile, however, clearly poses a modelling challenge, and, perhaps more importantly, is in obvious disagreement with practical observation.

To overcome these difficulties, constraints must be placed on the nature of the road's randomness. It has been suggested, and is now commonly agreed upon, that such appropriate constraints are achieved by assuming the entire road *surface* to be a realisation of a two-dimensional Gaussian homogenous and isotropic random process [12, 13].

A single road profile can therefore be conveniently represented by its PSD function, with the assumption of homogeneity (i.e., possessing statistical properties independent of coordinate *translations* [14]) making the direct spectral densities of the right and left tracks equal. The assumption of isotropy (i.e., possessing statistical properties independent of coordinate *rotations* [14]) renders the cross-spectra between the tracks equal and implies, somewhat conveniently, that they are dependent only on the vehicle track width and the single-track direct spectral density.

The nature of isotropy carries with it a number of implications limiting the specification of the direct spectral density and the reader is directed to the relevant literature [13-16] lest the assumption be applied haphazardly. For our present purposes, a permissible and sufficient form of the direct spectral density is the ubiquitous 'single slope' representation, often expressed in terms of κ , the spatial frequency:

$$S_D^{\xi}(\kappa) = c\left|\kappa\right|^{-2w} \tag{1}$$

The application of isotropy allows us to determine the road displacement spectral density matrix $\mathbf{S}^{\xi}$, which facilitates the calculation of the response spectral density matrix [17]:

$$\mathbf{S}^{R}(\omega) = \mathbf{H}^{*}(s)\mathbf{S}^{\xi}(\omega)\mathbf{H}^{T}(s) \tag{2}$$

where $\mathbf{H}$ is a matrix of the appropriate frequency response functions (FRFs) and the symbols * and ^{T} denote the complex conjugate and matrix transpose, respectively. The derivation of the FRFs matrix is explained in the next section.

SYSTEM EQUATIONS AND FREQUENCY RESPONSE FUNCTIONS

The equations of motion for the coupled half-car and hydraulic systems shown in the HIS vehicle in Figure 1 have been derived elsewhere [7] and are in the form:

$$\mathbf{M}\ddot{\mathbf{Y}} + \mathbf{C}\dot{\mathbf{Y}} + \mathbf{K}\mathbf{Y} = \mathbf{D}\mathbf{P} + \mathbf{F}_{ex} \tag{3}$$

$$\dot{\mathbf{P}} = \mathbf{N}\dot{\mathbf{Y}} + \mathbf{G}(s)\mathbf{P} \tag{4}$$

where the system state vectors are $\mathbf{Y} = \left[y_{wl}, y_{wr}, y, \theta\right]^T$ and $\mathbf{P} = \left[P_{Lr}, P_{Ul}, P_{Ll}, P_{Ur}\right]^T$. Present space limitations preclude a discussion of the various terms, but it will be sufficient here to note that $\mathbf{N}$ and $\mathbf{D}$ are hydraulic system-dependent constants, while $\mathbf{G}$ is dependent on both the hydraulic system and the complex frequency s and is derived using the linearised hydraulic impedance approach and the transfer matrix method.

After some manipulation, the FRFs matrix for the HIS vehicle is obtained:

$$\frac{\mathbf{Y}(s)}{\bar{\xi}(s)} = \mathbf{T}(s) = \left\{s^2\mathbf{M} + s\mathbf{C} + \mathbf{K} - s\mathbf{D}\left[s - \mathbf{G}(s)\right]^{-1}\mathbf{N}\right\}^{-1}\bar{\mathbf{F}}(s) \tag{5}$$

in which the displacement vector $\bar{\xi} = \left[\xi, 0, 0\right]^T = \left[\xi_l, \xi_r, 0, 0\right]^T$ and $\bar{\mathbf{F}}$ is a 4×4 matrix comprising all zero elements except the upper two diagonal terms $\bar{F}_{11}(s) = \bar{F}_{22}(s) = sc_t + k_t$.

The FRFs matrix for the conventional vehicle is found in a similar fashion. Upon setting $s = j\omega$, the FRFs describe the system displacement response to any harmonic road excitation.

The four FRFs (for each vehicle) corresponding to a left ground input are shown in Figure 2. Identical axes scales are used to enable a direct comparison between plots. It can be seen that the HIS vehicle behaves, as expected, almost exactly like the equivalent bounce car in the bounce mode and like the equivalent roll car in the roll mode. However, all three vehicles display distinctive behaviour in their wheel transmissibilities. For example, the left wheel FRFs show that the wheel hop modes (~9 Hz) are dominant with the (relatively soft) equivalent bounce car, while the sprung mass roll and bounce modes dominate the response curves for the HIS vehicle and (relatively stiff) equivalent roll vehicle, respectively.

Another point of note is that the right wheel FRFs (to left wheel input) are much higher with the HIS and equivalent roll vehicles than with the equivalent bounce vehicle. This is clearly a reflection of the fact that the stiffer roll vehicles transmit a greater level of motion to the opposite wheel while oscillating at their natural roll frequencies. But there is another interesting feature of the right wheel FRFs: the HIS response curve displays a much broader peak than that of the equivalent roll vehicle. This is a direct result of the interconnection system itself. That is, at frequencies above 5 Hz, an input at one wheel will be transmitted much more efficiently to the opposite wheel with the HIS vehicle than with the non-interconnected vehicles due to direct signal transmission through the hydraulic system.

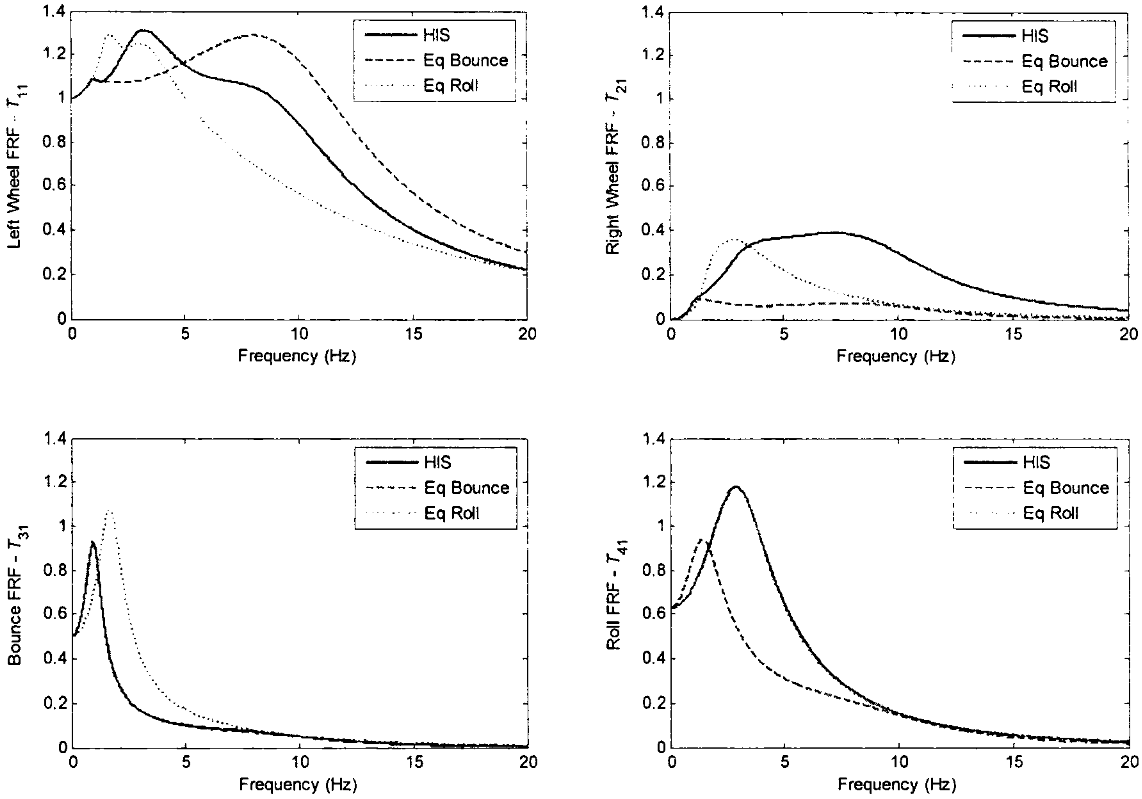

Figure 2: Displacement FRFs for left ground input

The FRFs matrices describe the ratio of output to input for harmonic system displacements. However, we are concerned here primarily with evaluating ride comfort, road holding and working space, which cannot be assessed directly through displacement FRFs alone. We are therefore required, before proceeding any further, to develop FRFs corresponding to the system outputs required for the performance indices outlined previously. The matrix form of these FRFs represents the $\mathbf{H}$ matrix in equation (2).

Given the displacement FRFs matrix, one may easily derive the acceleration, tyre force and deflection FRFs matrices, defined as:

$$\mathbf{T}^a(s) = \frac{s^2\mathbf{Y}(s)}{\xi(s)} \qquad \mathbf{T}^t(s) = \frac{\mathbf{F}_t(s)}{\xi(s)} \qquad \mathbf{T}^d(s) = \frac{\mathbf{Y}_d(s)}{\xi(s)} \tag{6}$$

in which $\mathbf{F}_t = [F_{tl}, F_{tr}]^T$ is the tyre dynamic normal force vector and $\mathbf{Y}_d = [y_{dl}, y_{dr}]^T$ is the suspension strut deflection vector.

We can now assemble the required FRFs matrix $\mathbf{H}$, such that:

$$\mathbf{Y}^R(s) = \mathbf{H}(s)\xi(s) \tag{7}$$

where

$$\mathbf{H} = \begin{bmatrix} T_{31}^a & T_{41}^a & T_{11}^t & T_{11}^d \\ T_{32}^a & T_{42}^a & T_{12}^t & T_{12}^d \end{bmatrix}^T \tag{8}$$

and the response vector, which contains the four variables used in the performance indices, is $\mathbf{Y}^R = \left[\ddot{y}, \ddot{\theta}, F_{tl}, y_{dl}\right]^T$, in which $F_{tl} = F_{tr}$ and $y_{dl} = y_{dr}$ due to the right-left vehicle symmetry. Equation (8) may be substituted into equation (2) to obtain the response spectral density matrix. The diagonal elements of this response matrix represent the direct spectral densities of the variables in $\mathbf{Y}^R$. It is these variables upon which the results in the following section are based, although the acceleration terms are frequency-weighted before evaluation [9].

RESULTS AND DISCUSSION

In this section, the vehicle PSD response is considered in the frequency domain up to 20 Hz. An 'average' road type is simulated ($w = 1.25$, $c = 50\times10^{-8}$ $\mathrm{m}^{0.5}\mathrm{cycle}^{1.5}$ [17]) at two vehicle speeds (*low speed* = 10 m/s, *high speed* = 30 m/s), although the effects of speed are not as evident here as has been found elsewhere [18], since the 'wheelbase filtering' phenomenon does not feature in the roll-plane model.

Figure 3 shows the vehicle response PSDs at low constant vehicle speed. As expected after observing the displacement FRFs in Figure 2, the HIS vehicle behaves very much like the equivalent bounce and roll vehicles in terms of the corresponding acceleration components. Thus the results indicate that in ride comfort the HIS car will perform better than the equivalent roll vehicle, but not as well as the equivalent bounce vehicle.

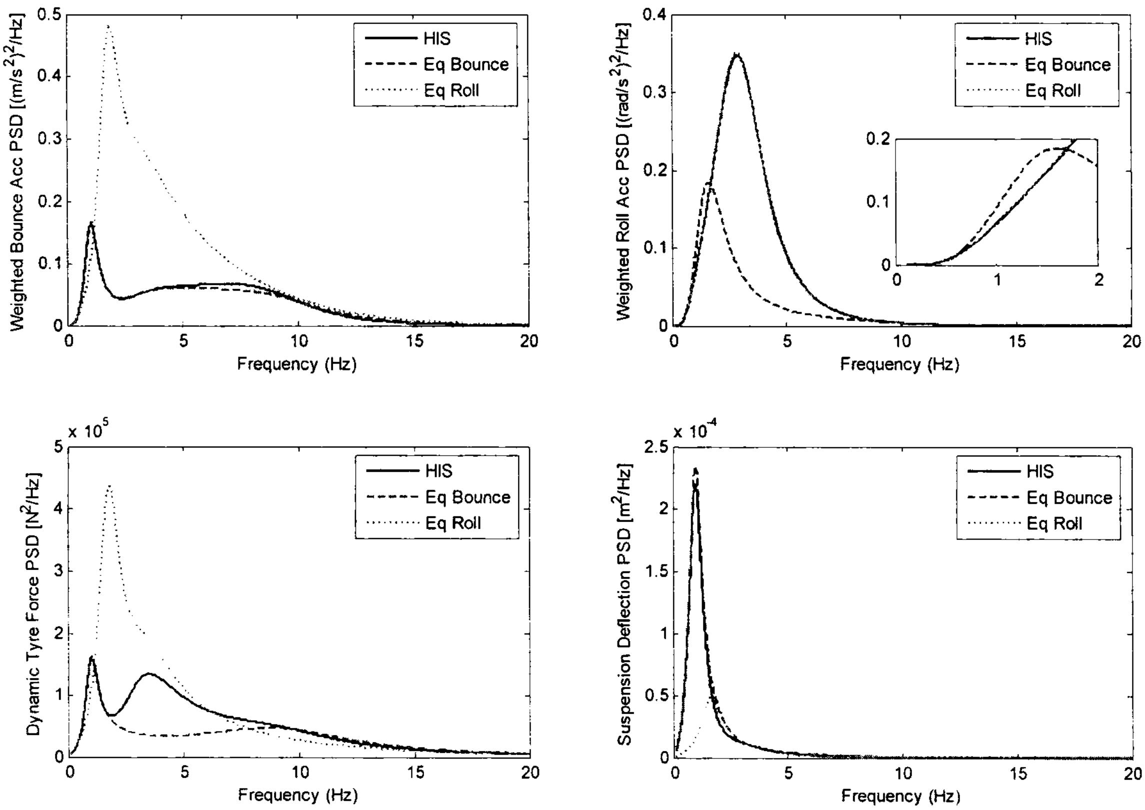

Figure 3: Vehicle response PSDs at low speed (10 m/s)

Figure 3 also indicates that the reduction in peak bounce acceleration has a large positive effect on the dynamic tyre force. The HIS vehicle clearly outperforms the equivalent roll vehicle in that respect. However, the HIS vehicle's large peak roll acceleration also adversely influences the tyre force, so the equivalent bounce vehicle performs better than the HIS vehicle in road holding. The suspension deflection plot shows that the HIS vehicle's working space is slightly better (smaller) than the equivalent bounce vehicle but significantly inferior to the equivalent roll vehicle. This illustrates that the bounce mode dominates the suspension deflection.

The absence of wheelbase filtering means the high speed response plots in Figure 4 show a very similar pattern to the low speed response, except that the magnitudes are significantly greater. One notable difference between the two responses is that the peak roll acceleration for all vehicles is smaller (in proportion to peak bounce acceleration) at high speed than at low speed and, consequently, the dynamic tyre force for the HIS vehicle in the 2–6 Hz range at high speed is closer to that of the equivalent bounce vehicle than is the case at low speed. It may also be noted that the peak roll acceleration for the equivalent bounce vehicle is larger (in proportion to the peak roll acceleration for the other vehicles) at low speed than at high speed.

Although the results in Figures 3 and 4 might indicate an ostensible superiority of the equivalent bounce vehicle in most respects, one must be careful in drawing broader conclusions. It is now well established that a vehicle with soft suspension is likely to exhibit relatively poor handling stability, and although the vehicle model used here neglects lateral dynamics, the results still indicate a soft-vehicle handling inferiority. Probably the best indicator of this is the 0–2 Hz range of the roll acceleration plots. Most handling manoeuvres occupy these frequencies, and it should not go unnoticed that the soft equivalent bounce vehicle performs relatively poorly throughout much of this range.

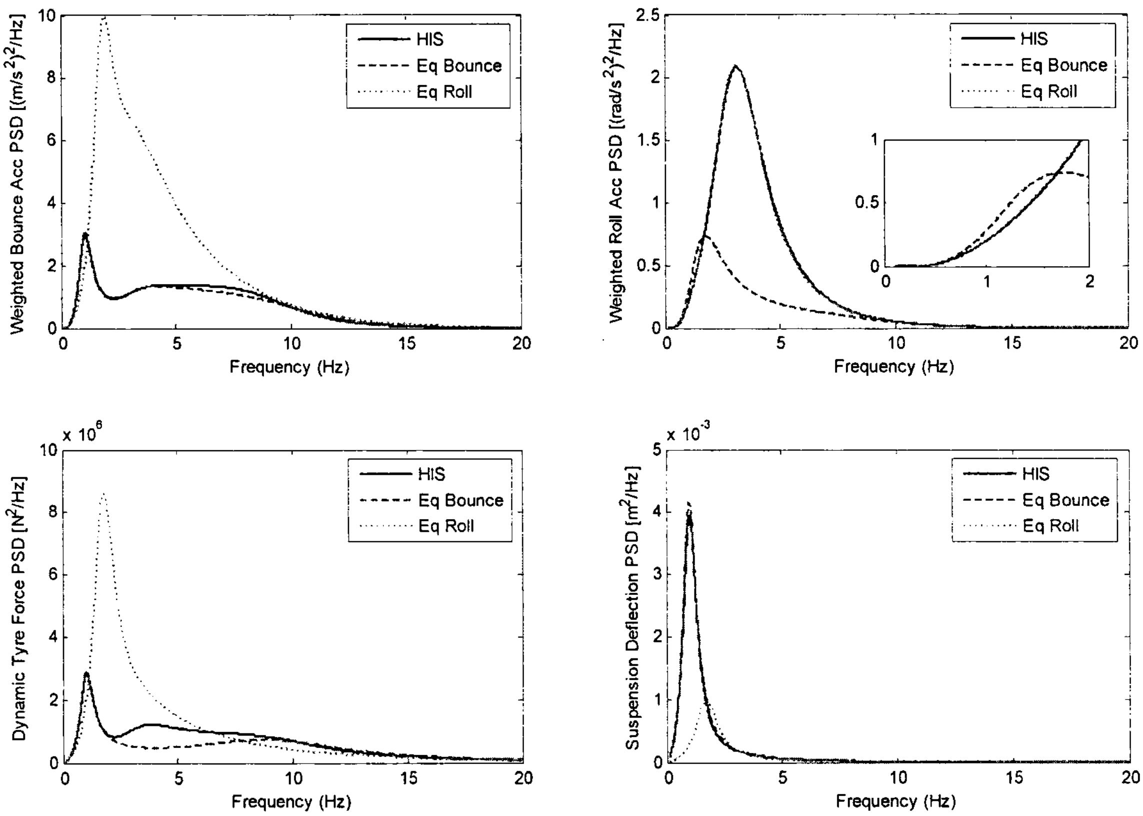

Figure 4: Vehicle response PSDs at high speed (30 m/s)

CONCLUSION

The results indicate that hydraulically interconnected suspension (HIS) systems provide a potentially viable method by which to partially overcome the ride/handling compromise. The 'typical' half-car model shows that added roll stiffness, which increases vehicle handling performance, may be attained with an HIS while maintaining better ride comfort and smaller tyre normal force fluctuations than would result if the increased roll stiffness was achieved with a stiffer conventional suspension. However, the working space advantages achieved with an HIS system are minimal and compare unfavourably with those of a stiff conventional suspension, due to the dominance of the bounce mode in the suspension deflection characteristics.

Recommendations for future work include the extension of the study to a full-car system, the use of other interconnection arrangements and model parameters, and the modelling of vehicle lateral dynamics to give a more thorough indication of handling performance.

REFERENCES

1. Smith, M. C. and Walker, G. W., "Interconnected Vehicle Suspension", Journal of Automobile Engineering, 219 (3), pp. 295-307, 2005.
2. Fontdecaba, J., "Integral Suspension System for Motor Vehicles Based on Passive Components", SAE Technical Paper Series, 2002-01-3105, 2002.
3. Wilde, J. R., Heydinger, G. J., Guenther, D. A., Mallin, T. and Devenish, A. M., "Experimental Evaluation of Fishhook Maneuver Performance of a Kinetic Suspension System", SAE Technical Paper Series, 2005-01-0392, 2005.
4. Jeyakumaran, J., Smith, W. and Zhang, N., "Transient Performance of a Hydraulically Interconnected Suspension System", Submitted to FISITA-2006 World Automotive Congress, Japan, 2006.
5. Liu, P. J., "An Analytical Study of Ride and Handling Performance of an Interconnected Vehicle Suspension", M.A.Sc. Thesis, Concordia University, 1994.
6. Ortiz, M., "Principles of Interconnected Suspensions", RaceCar Engineering, 7 (7-8), 1997.
7. Zhang, N., Smith, W. A. and Jeyakumaran, J., "Free Vibration of Vehicles with Hydraulically Interconnected Suspensions", In preparation, 2006.
8. Gobbi, M. and Mastinu, G., "Analytical Description and Optimization of the Dynamic Behaviour of Passively Suspended Road Vehicles", Journal of Sound and Vibration, 245 (3), pp. 457-481, 2001.
9. ISO 2631-1:1997 Evaluation of human exposure to whole-body vibration - Part 1: General requirements, 1997.
10. Mashadi, B. and Crolla, D. A., "Influence of ride motions on the handling behaviour of a passenger vehicle", Journal of Automobile Engineering, 219 (9), pp. 1047-1058, 2005.
11. Burton, A. W., Truscott, A. J. and Wellstead, P. E., "Analysis, modelling and control of an advanced automotive self-levelling suspension system", IEE Proc. Control Theory Appl., 142 (2), pp. 129-139, 1995.
12. Newland, D. E., "An Introduction to Random Vibrations and Spectral Analysis", Longman, 1975.
13. Dodds, C. J. and Robson, J. D., "The Description of Road Surface Roughness", Journal of Sound and Vibration, 31 (2), pp. 175-183, 1973.

14. Heath, A. N., "Application of the Isotropic Road Roughness Assumption", Journal of Sound and Vibration, 115 (1), pp. 131-144, 1987.
15. Kamash, K. M. A. and Robson, J. D., "The Application of Isotropy in Road Surface Modelling", Journal of Sound and Vibration, 57 (1), pp. 89-100, 1978.
16. Kamash, K. M. A. and Robson, J. D., "Implications of Isotropy in Random Surfaces", Journal of Sound and Vibration, 54 (1), pp. 131-145, 1977.
17. Robson, J. D., "Road Surface Description and Vehicle Response", International Journal of Vehicle Design, 1 (1), pp. 25-35, 1979.
18. Cossalter, V., Doria, A., Garbin, S. and Lot, R., "Frequency-domain method for evaluating the ride comfort of a motorcycle", Vehicle System Dynamics, 44 (4), pp. 339-355, 2006.

Acknowledgments

Financial support for this research was provided jointly by the Australian Research Council (ARC LP0562440) and the University of Technology, Sydney.